www.sciencemag.org/cgi/content/full/science.1254445/DC1

Supplementary Materials for

Prevention of muscular dystrophy in mice by CRISPR/Cas9–mediated editing of germline DNA

Chengzu Long, John R. McAnally, John M. Shelton,
Alex A. Mireault, Rhonda Bassel-Duby, Eric N. Olson*

*Corresponding author. E-mail: eric.olson@utsouthwestern.edu

Published 14 August 2014 on *Science* Express
DOI: 10.1126/science.1254445

This PDF file includes:

Materials and Methods

Plasmids. The hCas9 plasmid (Addgene plasmid 41815) containing the human codon optimized Cas9 gene and the gRNA Cloning Vector plasmid (Addgene plasmid 41824) containing the backbone of sgRNA were purchased from Addgene. Cloning of sgRNA was done according to the Church Lab CRISPR plasmid instructions (http://www.addgene.org/crispr/church/).

In vitro transcription of Cas9 mRNA and sgRNA. T3 promoter sequence was added to the hCas9 coding region by PCR. T3-hCas9 PCR product was gel purified and subcloned into pCRII-TOPO vector (Invitrogen) according to the manufacturer's instructions. Linearized T3-hCas9 plasmid was used as the template for in vitro transcription using the mMESSAGE mMACHINE T3 Transcription Kit (Life Technologies). T7 promoter sequence was added to the sgRNA template by PCR. The gel purified PCR products were used as template for in vitro transcription using the MEGAshortscript T7 Kit (Life Technologies). hCas9 RNA and sgRNA were purified by MEGAclear kit (Life Technologies) and eluted with nuclease-free water (Ambion). The concentration of RNA was measured by a NanoDrop instrument (Thermo Scientific).

Single-stranded oligodeoxynucleotide (ssODN). ssODN was used as HDR template and purchased from Integrated DNA Technologies as Ultramer DNA Oligonucleotides. ssODN was mixed with Cas9 mRNA and sgRNA directly without purification. The sequence of ssODN is listed in **table S1**.

CRISPR/Cas9-mediated genomic editing by one-cell embryo injection. All animal procedures were approved by the Institutional Animal Care and Use Committee at the

University of Texas Southwestern Medical Center. B6C3F1 (C57BL/6NCr female X C3H/HeN MTV male), C57BL/6NCr, and C57BL/10ScSn-*Dmd*^{mdx}/J were three mouse strains used as oocyte donors. Superovulated female B6C3F1 mice (6 weeks old) were mated to B6C3F1 stud males. Superovulated female C57BL/6NCr females (12-18 grams) were mated to C57BL/6NCr males and superovulated female homozygote C57BL/10ScSn-*Dmd*^{mdx}/J (12-18 grams) were mated to hemizygote C57BL/10ScSn-*Dmd*^{mdx}/J stud males. Zygotes were harvested and kept in M16 medium (Brinster's medium for ovum culture with 100U/ml penicillin and 50 mg/ml streptomycin) at 37^{o}C for 1 hour. Zygotes were transferred to M2 medium (M16 medium and 20 mM HEPES) and injected with hCas9 mRNA, sgRNA and ssODN. Cas9/sgRNA was injected into the pronucleus only (termed Nuc) or pronucleus and cytoplasm (termed Nuc+Cyt). Different doses of Cas9 mRNA, sgRNA and ssODNs were injected into zygotes by Nuc or Nuc+Cyt (as detailed in **table S2**). Injected zygotes were cultured in M16 medium for 1 hour at 37^{o}C and then transferred into the oviducts of pseudopregnant ICR female mice.

Isolation of genomic DNA. Tail biopsies were added to 100µl of 25mM NaOH / 0.2 mM EDTA solution and placed at 95ºC for 15 min and then cooled to room temperature. Following the addition of 100µl of 40 mM Tris-HCl (pH 5.5), the tubes were centrifuged at 15,000 x g for 5 minutes. DNA samples were kept at 4ºC for several weeks or at –20ºC for long-term storage. Genomic DNA was isolated from muscle using TRIzol (Life Technologies) according to the manufacturer's instructions.

Amplifying the target genomic region by PCR. PCR assays contained 2 µl of GoTaq (Promega), 20 µl of 5X Green GoTaq Reaction Buffer, 8 µl of 25mM $MgCl_2$, 2µl of 10µM primer (DMD729F and DMD729R) **(table S1)**, 2µl of 10mM dNTP, 4 µl of genomic DNA,

and ddH_2O to 100 µl. PCR conditions were: 94ºC for 2 min; 32X (94ºC for 15 sec, 59ºC for 30 sec, 72ºC for 1 min); 72ºC for 7 min; followed by 4ºC. PCR products were analyzed by 2% agarose gel electrophoresis and purified from the gel using the QIAquick PCR Purification Kit (Qiagen) for direct sequencing. These PCR products were subcloned into pCRII-TOPO vector (Invitrogen) according to the manufacturer's instructions. Individual clones were picked and the DNA was sequenced.

RFLP analysis of PCR products. Digestion reactions consisting of 20 µl of genomic PCR product, 3 µl of 10X NEB buffer CS, and 1 µl of TseI (New England BioLabs) were incubated for 1 hour at 65ºC and analyzed by 2% agarose gel electrophoresis. Digested PCR product from wild-type DNA is 581bp, while HDR-mediated genomic editing DNA from F_0 mice shows an additional product at approximately 437bp.

T7E1 analysis of PCR products. Mismatched duplex DNA was obtained by denaturation/renaturation of 25 µl of the genomic PCR samples using the following conditions:

95ºC for 10 min, 95ºC to 85ºC (-2.0ºC/s), 85ºC for 1 min, 85ºC to 75ºC (-0.3ºC/s), 75ºC for 1 min, 75ºC to 65ºC (-0.3ºC/s), 65ºC for 1 min, 65ºC to 55ºC (-0.3ºC/s), 55ºC for 1 min, 55ºC to 45ºC (-0.3ºC/s), 45ºC for 1 min, 45 ºC to 35 ºC (-0.3ºC/s), 35ºC for 1 min, 35ºC to 25ºC (-0.3ºC/s), 25ºC for 1 min, hold at 4ºC.

Following denaturation/renaturation, the following was added to the samples: 3 µl of 10X NEB buffer 2, 0.3 µl of T7E1 (New England BioLabs), and ddH_2O to 30 µl. Digestion reactions were incubated for 1 hour at 37ºC. Undigested PCR samples and

T7E1 digested PCR products were analyzed by 2% agarose gel electrophoresis. Undigested PCR product is 729bp, while genomic DNA from F_0 mice with mismatched DNA showed two additional digestion products at approximately 440bp and 290bp.

Grip strength test. Muscle strength was assessed by a grip strength behavior task performed by the Neuro-Models Core Facility at UT Southwestern Medical Center. The mouse was removed from the cage, weighed and lifted by the tail causing the forelimbs to grasp the pull-bar assembly connected to the grip strength meter (Columbus Instruments). The mouse was drawn along a straight line leading away from the sensor until the grip is broken and the peak amount of force in grams was recorded. This was repeated 5 times.

Serum creatine kinase (CK) measurement. Blood was collected from the submandibular vein and serum CK level was measured by VITROS Chemistry Products CK Slides to quantitatively measure CK activity using VITROS 250 Chemistry System.

Histological analysis of muscles. Skeletal muscle from wild-type, *mdx*, and corrected *mdx-C* mice were individually dissected and cryoembedded in a 1:2 volume mixture of Gum Tragacanth powder (Sigma-Aldrich) to Tissue Freezing Medium (TFM) (Triangle Bioscience). Hearts were cryoembedded in TFM. All embeds were snap frozen in isopentane heat extractant supercooled to -155°C. Resulting blocks were stored overnight at -80°C prior to sectioning. Eight-micron transverse sections of skeletal muscle, and frontal sections of heart were prepared on a Leica CM3050 cryostat and air-dried prior to same day staining. H&E staining was performed according to established staining protocols and dystrophin immunohistochemistry was performed

using MANDYS8 monoclonal antisera (Sigma-Aldrich) with modifications to manufacturer's instructions. In brief, cryostat sections were thawed and rehydrated/delipidated in 1% triton/phosphate-buffered-saline, pH 7.4 (PBS). Following delipidation, sections were washed free of Triton, incubated with mouse IgG blocking reagent (M.O.M. Kit, Vector Laboratories), washed, and sequentially equilibrated with MOM protein concentrate/PBS, and MANDYS8 diluted 1:1800 in MOM protein concentrate/PBS. Following overnight primary antibody incubation at 4°C, sections were washed, incubated with MOM biotinylated anti-mouse IgG, washed, and detection completed with incubation of Vector fluorescein-avidin DCS. Nuclei were counterstained with propidium iodide (Molecular Probes) prior to cover slipping with Vectashield.

Imaging and analysis. Specimens were reviewed with a Zeiss Axioplan 2iE upright photomicroscope equipped with epifluiorescence illumination, CRI color wheel, and Zeiss Axiocam monochromatic CCD camera. OpenLab 4.0 acquisition and control software (Perkin-Elmer) was used to capture 10x and 20x objective magnification fields, and further used to apply indexed pseudocoloring and merge image overlays. Images were peak levels-adjusted with Adobe Photoshop CS2 and saved for image analysis. ImageJ 1.47 was used to apply stereologic morphometric randomization grid overlays and the software's counting functions used to mark and score approximately 500 aggregate myofibers (from a minimum of three interval-sections) for dystrophin positive and negative immunostaining from each muscle group. H&E stained sections of soleus muscle for each genotype were further analyzed with ImageJ 1.47 for size and characteristic. In brief, sarcolemmal boundaries of 115+ stereologically randomized

myofibers were manually delineated, their cross sectional area calculated, and central-nuclear phenotype recorded.

Western blot analysis. Muscles were dissected and rapidly frozen in liquid nitrogen. Protein extraction and western blot analysis were performed as described (*34, 35*) with modification. Samples were homogenized with a homogenizer (POLYTRON System PT 1200 E) for 2 X 20 seconds in 400 µL sample buffer containing 10%SDS, 62.5 mM Tris, 1mM EDTA and protease inhibitor (Roche). Protein concentration was measured using the BCA Protein Assay Kit (Pierce). Fifty micrograms of protein from each muscle sample was loaded onto a gradient SDS-PAGE (Bio-Rad). The gel was run at 100V for 2.5 hours. Separated proteins were transferred to a PVDF membrane at 35V overnight in a cold room (4^{o}C). The PVDF membrane was stained for total protein using 2% Ponceau Red and then blocked for one hour with 5% w/v nonfat dry milk, 1X TBS, 0.1% Tween-20 (TBST) at 25°C with gentle shaking. The blocked membrane was incubated with a mouse anti-dystrophin monoclonal antibody (MANDYS8, Sigma-Aldrich, 1: 1,000 dilution in 5% milk/TBST) overnight at 4°C and then washed in TBST. The blot was then incubated with horseradish peroxidase conjugated goat anti-mouse IgG secondary antibody (Bio-Rad, 1:10,000 dilution) for one hour at 25°C. After washing with TBST, the blot was exposed to Western Blotting Luminol Reagent (Santa Cruz Biotech) for 1 min to detect signal. Protein loading was monitored by anti-GAPDH antibody (Millipore, 1:10,000 dilution).

Deep sequencing of off-target sites. Off-target loci were amplified by PCR using primers listed in **table S1** for (A) *mdx* (B) *mdx*+Cas9 (C) WT and (D) WT+Cas9. PCR products were purified by MinElute PCR purification kit (QIAGEN), adjusted to the same

concentration (10 ng/μL), and equal volumes (5 μL) were combined for each group. Library preparation was performed according to the manufacturer's instructions (KAPA Library Preparation Kits with standard PCR library amplification module, Kapa Biosystems). Sequencing was performed on the Hiseq 2500 from Illumina and was run using Rapid Mode 150PE chemistry. Sequencing reads were mapped using BWA (http://bio-bwa.sourceforge.net/). Reads with mapping quality greater than 30 were retained for variant discovery. The mean read depth across all regions and all samples was 2570-fold. The variants were called using SAMtools (http://samtools.sourceforge.net/) plus custom scripts. In each region, insertion and deletion of 3 base pairs or longer were counted in a 50-bp window centered on the Cas9 potential cleavage sites.

Laser microdissection of satellite cells. Frozen sections from cryoembedments of gastrocnemius were mounted onto polyethylene membrane frame slides (Leica Microsystems PET-Foil 11505151) for same-day set-up of Pax-7 immunohistochemistry. Monoclonal Pax-7 antibody (Developmental Studies Hybridoma Bank) was used as described (*36*) with modifications to antigen retrieval for working with PET-foil membrane frame slides (*37*). In brief, gastrocnemius cryosections were air-dried, fixed with 4% paraformaldehyde, Triton-X100 delipidated and incubated in antigen-retrieval buffer (sodium citrate buffer pH 6.0) at 65°C for 20 hours. Following antigen retrieval, sections were quenched free of endogenous peroxidases with 0.6% hydrogen peroxide, and incubated with mouse IgG blocking reagent (M.O.M. Kit, Vector Laboratories), washed with PBS, incubated with MOM protein concentrate/PBS, and followed by overnight incubation with Pax-7 antibody (2 μg/ml) in MOM protein

concentrate/PBS at 4°C. Sections were washed with PBS and incubated with MOM biotinylated anti-mouse IgG, streptavidin-peroxidase (Vector Laboratories), and color developed with diaminobenzidine chromagen (DAB, Dako). Nuclei were counterstained with nuclease-free Mayer's hematoxylin. Pax-7 positive satellite cells were microscopically identified and isolated by laser microdissection at 63x objective magnification using a Leica AS-LMD. Sixty to seventy Pax-7 positive satellite cells were isolated for each genotype and pooled into 10µl of capture buffer (DirectPCR Lysis Reagent, Viagen Biotech Inc.) and stored at -20°C. The target genomic region was amplified by PCR using primers DMD232_f and DMD232_r **(table S1)**, as described above.

Supplementary Materials References

34. L. V. Nicholson *et al.*, *J Neurol Sci* **94**, 125-136 (1989).

35. K. Kodippili *et al.*, *PLoS One* **9**, e88280 (2014).

36. M. M. Murphy, J. A. Lawson, S. J. Mathew, D. A. Hutcheson, G. Kardon, *Development* **138**, 3625-3637 (2011).

37. L. M. Gjerdrum, I. Lielpetere, L. M. Rasmussen, K. Bendix, S. Hamilton-Dutoit, *J Mol Diagn* **3**, 105-110 (2001).

Supplementary Figures

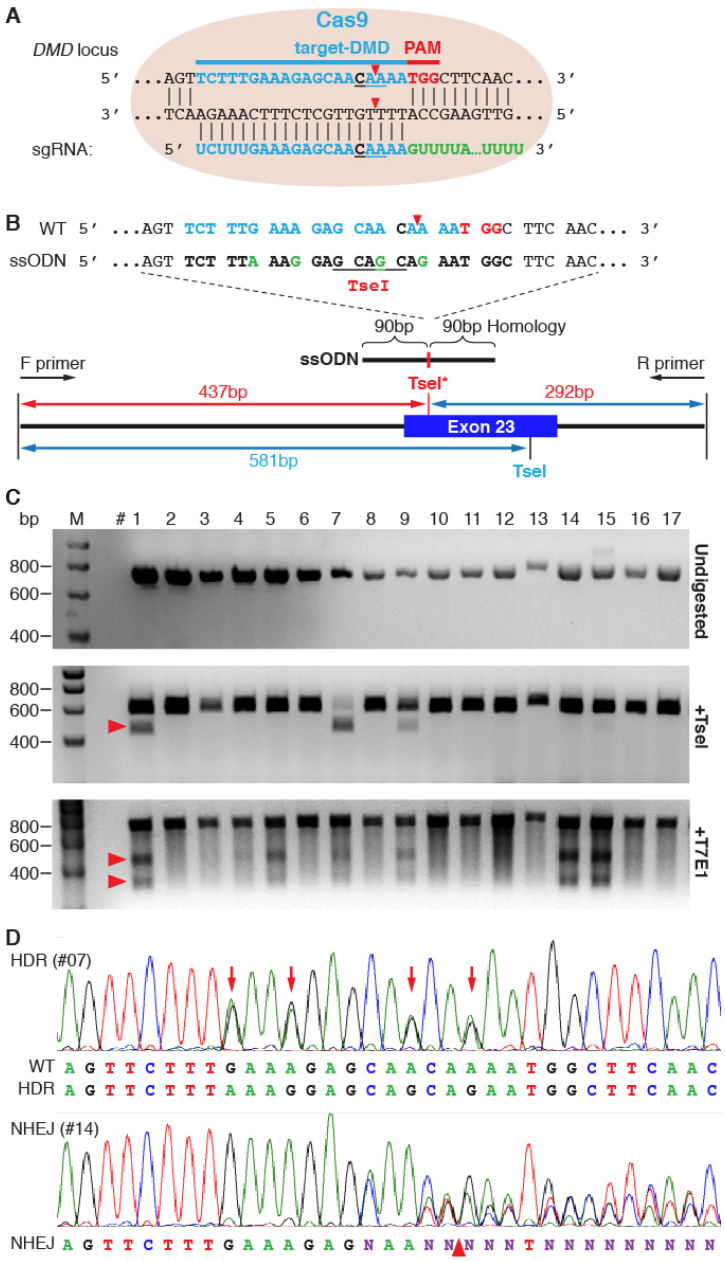

Fig. S1. HDR- and NHEJ-mediated gene editing of *Dmd* in wild-type mice.

(A) Schematic of the 20-nt sgRNA target sequence of *Dmd* (blue) and the PAM (red). Red arrowhead indicates Cas9 cleavage site. Green nucleotides mark the sgRNA scaffold.

(B) Strategy of PCR-based genotyping. ssODN, which contains 90 bp of homology sequence flanking each side of the target site was used as HDR template. ssODN incorporates four silent mutations (green) that eliminate re-cutting by the sgRNA/Cas9 complex and adds a TseI restriction enzyme site (underlined) for genotyping and quantification of HDR-mediated gene editing. Black arrows indicate the positions of the PCR primers corresponding to the *Dmd* gene editing site. Digestion of the PCR product (729 bp) with TseI reveals the occurrence of HDR (437 bp).

(C) (Upper panel) PCR-based genotyping using DNA isolated from tail biopsies of 17 mouse pups from one litter (**table S2**) with primers listed in **table S1**. (Middle panel) The PCR products were cut with TseI for restriction fragment length polymorphism (RFLP) analysis to screen for HDR. (Lower panel) T7 endonuclease I (T7E1), which is specific to heteroduplex DNA caused by CRISPR/Cas9-mediated genome editing, was used to screen for mutations. DNA products were loaded on a 2% agarose gel. Red arrowhead indicates cleavage bands of TseI or T7E1. M denotes size marker lane. bp indicates the base pair length of the marker bands.

(D) Sequencing results of PCR product of (upper panel) mouse #07 (from **fig. S1C**) showing HDR and of (lower panel) mouse #14 (from **fig. S1C**) showing NHEJ-mediated editing of the *Dmd* gene. Red arrows indicate the location of the point mutations introduced by HDR. Red arrowhead points to the mixed sequencing peaks on

chromatograms near the targeted site indicating heterozygous NHEJ-mediated gene editing.

(E) Sequence of *Dmd* alleles from four F_0 mice (#07, #13, #14 and #15 from **fig. S1C**) from microinjection of Cas9, sgRNA and ssODN into B6C3F1 mouse zygotes. PCR products from genomic tail DNA of each mouse were subcloned into pCRII-TOPO vector and individual clones were picked and sequenced. Silent mutations are indicated with green letters. Point mutations are indicated with red letters. Red lower case letters are the inserted sequences at the site indicated by the red arrowhead. Deleted sequences are replaced by black dashes. The genotype of each genomic DNA clone is listed next to the sequence and in-frame insertions or deletions are labeled in blue (termed IF-Ins. and IF-Del.). The number of inserted nucleotides is indicated by (+) and the deletion is indicated with (-). The number (No.) of clones with identical sequence is indicated by (×).

A

*Dmd*_Ex23

mdx 5′ ...AGT TCT TTG AAA GAG CAA TAA AAT GGC TTC AAC... 3′
N-Ser-Ser-Leu-Lys-Glu-Gln- *

WT 5′ ...AGT TCT TTG AAA GAG CAA CAA AAT GGC TTC AAC... 3′
N-Ser-Ser-Leu-Lys-Glu-Gln-Gln-Asn-Gly-Phe-Asn-C

HDR 5′ ...AGT TCT TTA AAG GAG CAG CAG AAT GGC TTC AAC... 3′
N-Ser-Ser-Leu-Lys-Glu-Gln-Gln-Asn-Gly-Phe-Asn-C

NHEJ 5′ ...AGT TCT TTG AAA GAG CAA --- AAT GGC TTC AAC... 3′(-3bp)
N-Ser-Ser-Leu-Lys-Glu-Gln-----Asn-Gly-Phe-Asn-C (-1A.A.)

B

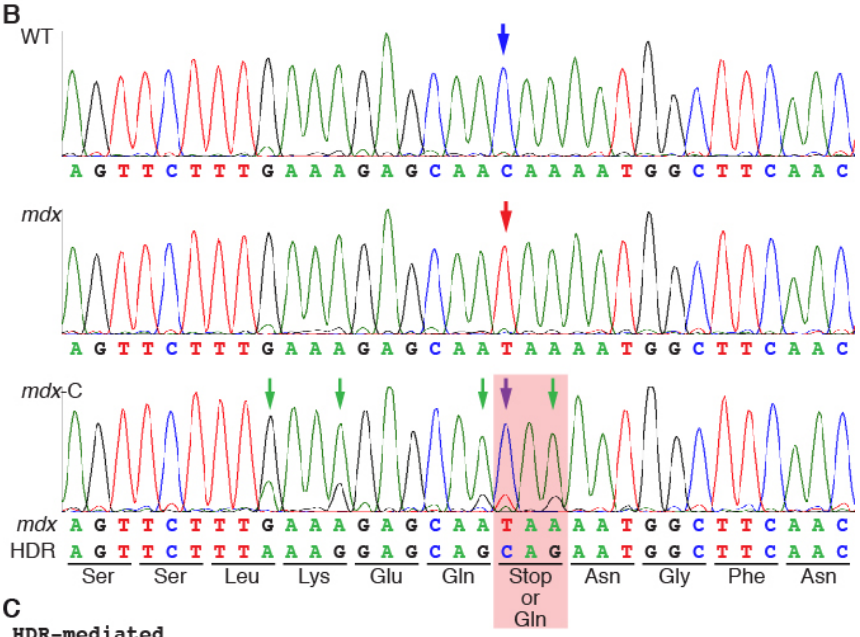

C

HDR-mediated correction	**Sequence**	**Mutation**	**No.**
mdx-C1	AGTTCTTTGAAAGAGCAATAAAATGGCTTCAAC	*mdx*	×13
	AGTTCTTTAAAGGAGCAGCAGAATGGCTTCAAC	HDR	×12
mdx-C2	AGTTCTTTGAAAGAGCAATAAAATGGCTTCAAC	*mdx*	×23
	AGTTCTTTAAAGGAGCAGCAGAATGGCTTCAAC	HDR	×1
mdx-C3	AGTTCTTTGAAAGAGCAATAAAATGGCTTCAAC	*mdx*	×17
	AGTTCTTTAAAGGAGCAGCAGAATGGCTTCAAC	HDR	×5
mdx-C4	AGTTCTTTGAAAGAGCAATAAAATGGCTTCAAC	*mdx*	×17
	AGTTCTTTAAAGGAGCAGCAGAATGGCTTCAAC	HDR	×5
mdx-C5	AGTTCTTTGAAAGAGCAATAAAATGGCTTCAAC	*mdx*	×3
	AGTTCTTTAAAGGAGCAGCAGAATGGCTTCAAC	HDR	×3
mdx-C6	AGTTCTTTGAAAGAGCAATAAAATGGCTTCAAC	*mdx*	×0
	AGTTCTTTAAAGGAGCAGCAGAATGGCTTCAAC	HDR	×6
mdx-C7	AGTTCTTTGAAAGAGCAATAAAATGGCTTCAAC	*mdx*	×5
	AGTTCTTTAAAGGAGCAGCAGAATGGCTTCAAC	HDR	×4

NHEJ-mediated correction			
mdx-N1	AGTTCTTTGAAAGAGCAATAAAATGGCTTCAAC	*mdx*	×2
	AGTTCTTTGAA----------TGGCTTCAAC	IF-Del.(-12)	×10(83%)
mdx-N2	AGTTCTTTGAAAGAGCAATAAAATGGCTTCAAC	*mdx*	×7
	AGTTCTTTG------CA---AAATGGCTTCAAC	IF-Del.(-9)	×4 (36%)
mdx-N3	AGTTCTTTGAAAGAGCAATAAAATGGCTTCAAC	*mdx*	×8
	AGTTCTTTGAAAGA-A-------//-----CCT	IF-Del.(-48)	×2 (20%)
mdx-N4	AGTTCTTTGAAAGAGCAATAAAATGGCTTCAAC	*mdx*	×3
	AGTTCTTTGAAAGAGCAA---AATGGCTTCAAC	IF-Del.(-3)	×3 (43%)
	AGTTCTTTGAAAGAGTAATAAAATGGCTTCAAC	Point	×1

Fig. S2. HDR- and NHEJ-mediated gene correction in *mdx* mice.

(A) Schematic illustrating CRISPR/Cas9-mediated gene correction via HDR or NHEJ. The corresponding amino acid residues are shown under the DNA sequence.

(B) Direct sequencing results of WT, *mdx* and corrected *mdx*-C mice. Blue arrow indicates the WT allele (upper). Red arrow indicates the *mdx* allele (middle). Purple arrow indicated the corrected allele mediated by HDR. Green arrows indicate the silent mutation sites (lower). The corresponding amino acid residues are shown under the DNA sequence. Red box indicates the corrected site.

(C) Sequence of *Dmd* alleles present in F_0 *mdx*-C mice (**Fig. 1E**) from microinjection of Cas9, sgRNA and ssODN into *mdx* mouse (C57BL/10ScSn-*Dmd*^{mdx}/J) zygotes. PCR products from genomic tail DNA of each mouse were subcloned into pCRII-TOPO vector and individual clones were picked and sequenced. The *mdx* point mutation (C to T) is marked in red. Silent mutations are indicated with green letters. The number (No.) of clones with identical sequence is indicated by (×). The variability observed in the ratio of HDR or NHEJ sequence to *mdx* sequence for each *mdx*-C mouse reflects the degree of mosaicism.

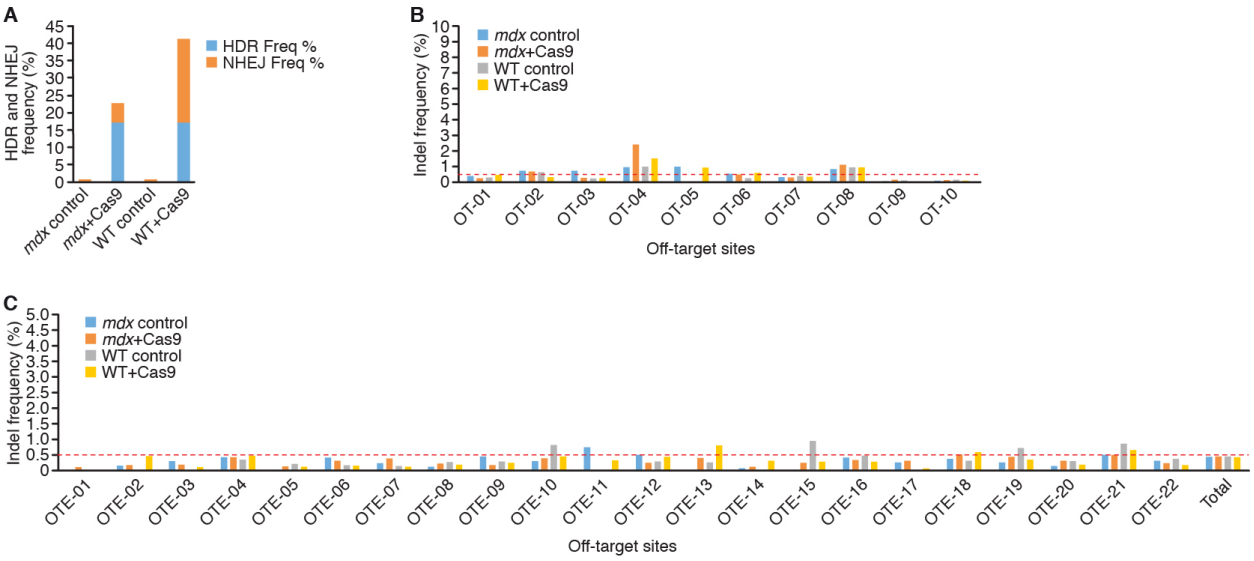

Fig. S3. Deep sequencing analysis of target site (*Dmd*) and 32 theoretical off-target sites.

(A) Frequency of HDR- and NHEJ-mediated gene correction at target site (*Dmd*) from deep sequencing of DNA from four groups of mice: *mdx*, *mdx*+Cas9, WT and WT+Cas9.

(B) Frequency of NHEJ-mediated indels at genome-wide “top ten” theoretical off-target sites (OT-01 to OT-10) (**table S3**) from deep sequencing results of DNA from the four groups of mice.

(C) Frequency of NHEJ-mediated indels at twenty-two theoretical off-target sites within exons (OTE-01 to OTE-22) (**table S3**) from deep sequencing of DNA from the four groups of mice.

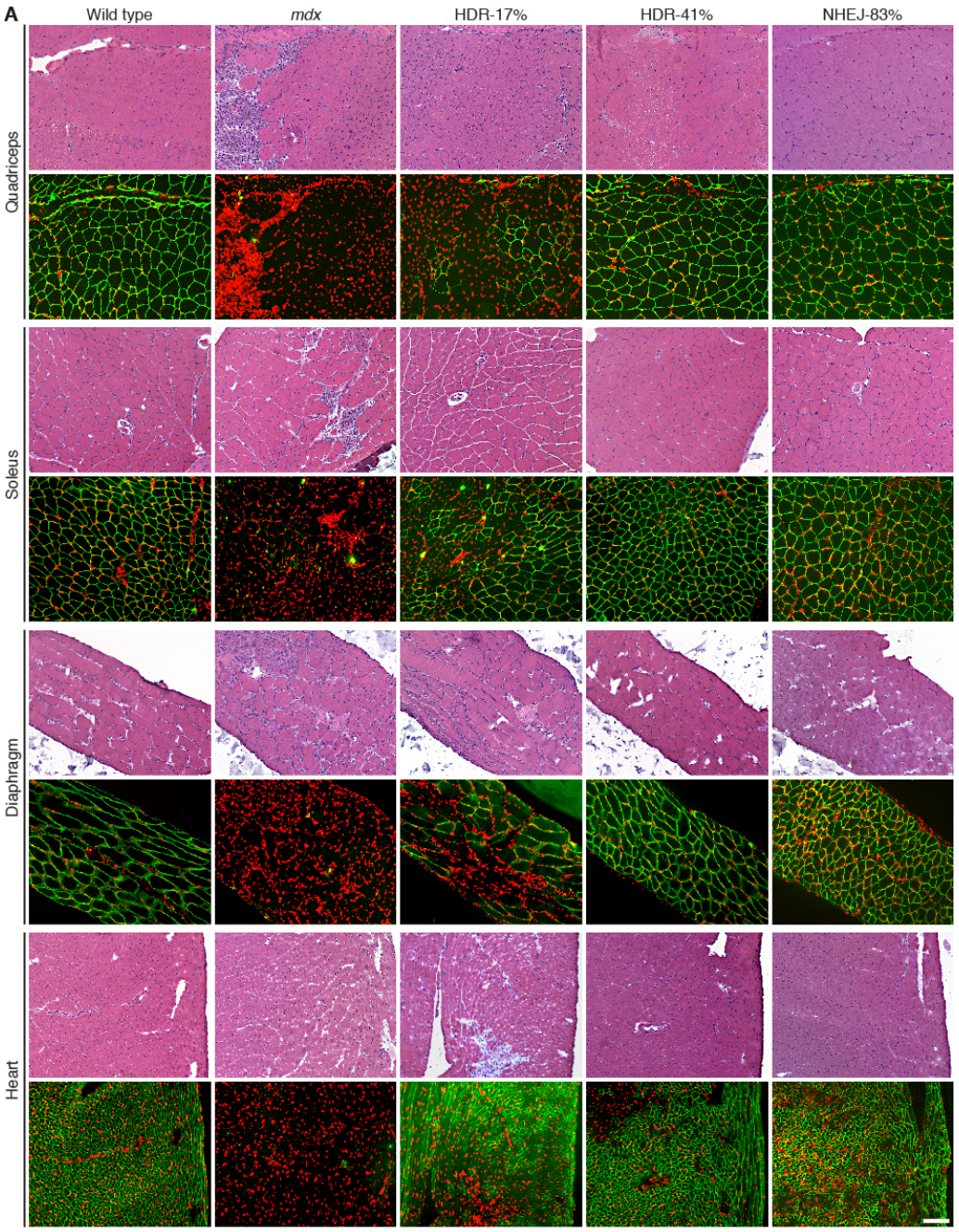
A
Wild type
mdx
HDR-17%
HDR-41%
NHEJ-83%
Quadriceps
Soleus
Diaphragm
Heart
B
Heart
Quadriceps
kD
M
WT
mdx
Partially
Fully
250
150
100
75
Anti-Dystrophin
Anti-GAPDH
37
Ponceau Red

Fig. S4. Histological and Western blot analysis of muscle from wild-type, *mdx*, and *mdx*-C mice.

(A) Hematoxylin and eosin (H&E) and immunostaining of muscles from 7-9 week old wild-type, *mdx, and mdx-C* mice (HDR-17%, HDR-41% and NHEJ-83% corrected allele; as seen in **Fig. 2**). Immunofluorescence (green) detects dystrophin. Nuclei are labeled by propidium iodide (red). Scale bar, 100 microns.

(B) Western blot analysis of heart and skeletal muscle (quadriceps) samples from wild-type, *mdx*, and partially corrected (HDR-17%) and fully corrected (HDR-41%) *mdx*-C mice. Red arrowhead (>250kD) indicates the immunoreactive bands of dystrophin. Lower bands (<250kD), which were also absent in *mdx* samples, likely represent proteolytic breakdown of full-length dystrophin protein, natural variants or protein synthesis intermediates. The same pattern of bands was observed in samples from wild-type and *mdx*-C mice. GAPDH is a loading control. PVDF membrane was stained for total protein by 2% Ponceau Red. M denotes size marker lane. kD indicates the protein length of the marker bands.

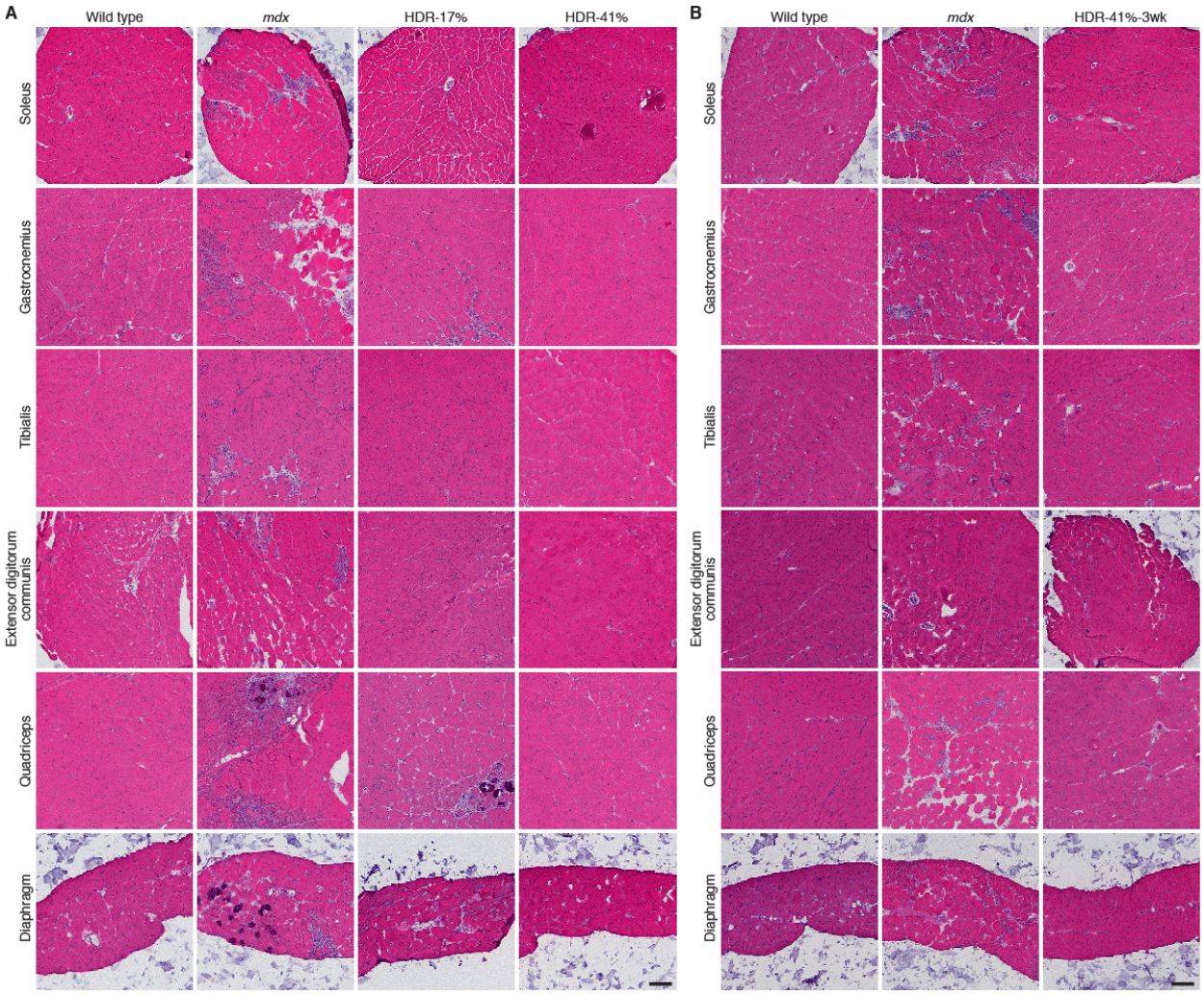

Fig. S5. Histology of muscles showing decrease in fibrosis and necrosis by CRISPR/Cas9-mediated genomic editing of *Dmd* allele.

Hematoxylin and eosin (H&E) stained transverse cryosections of whole soleus, gastrocnemius, tibialis-anterior, extensor-digitorum-communis, quadriceps, and diaphragm from **(A)** 7-9 week old wild-type, *mdx*, HDR-17% and HDR-41% and **(B)** 3-week old wild-type, *mdx*, HDR-40%-3wk. Scale bar, 125 microns.

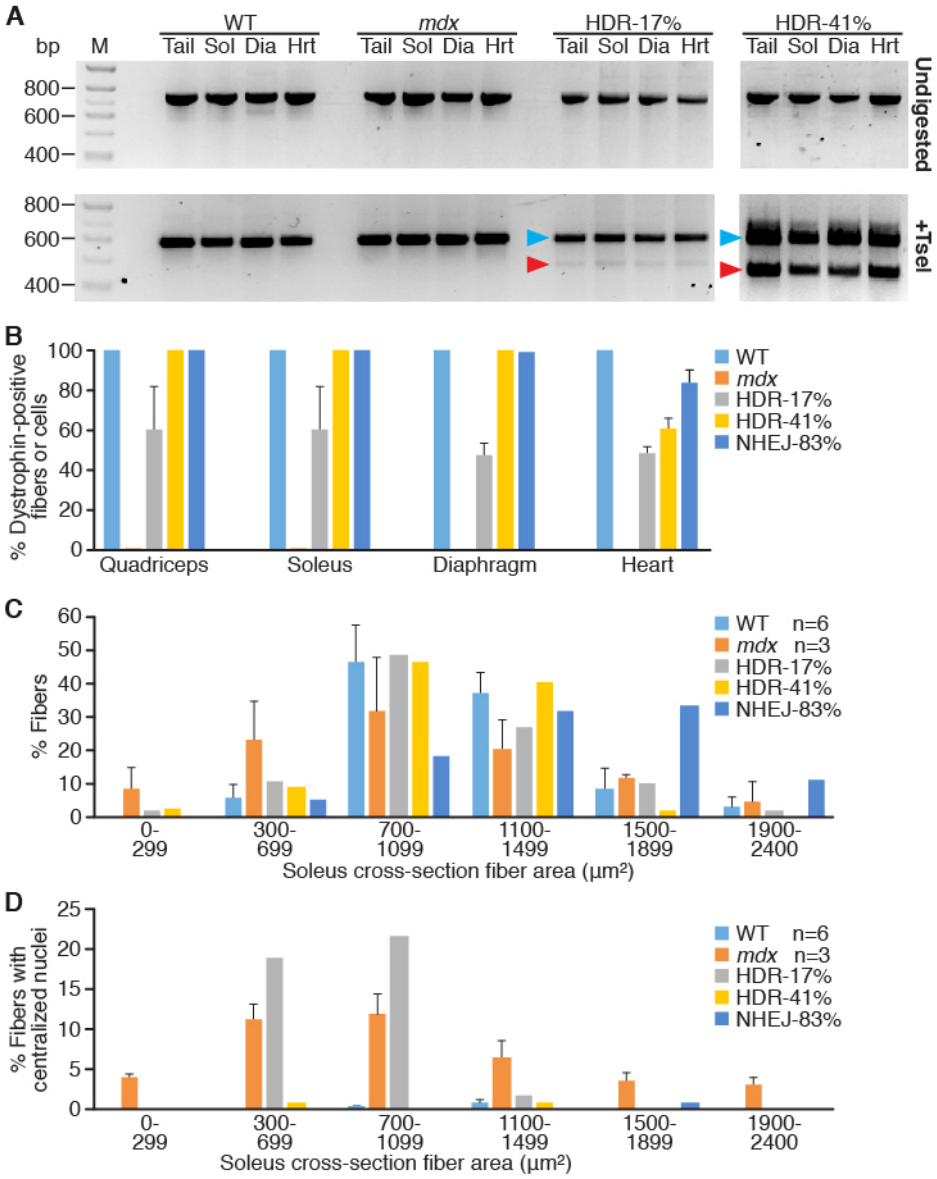

Fig. S6. RFLP analysis and myofiber measurements of muscle from wild-type, *mdx*, and corrected *mdx*-C mice.

(A) RFLP analysis to quantify the degree of mosaicism of genomic DNA isolated from tail, soleus (Sol), diaphragm (Dia) and heart (Hrt) of wild-type, *mdx*, HDR-17% and HDR-41% mice. PCR was performed using genomic DNA using primers (Dmd729F and Dmd729R) (upper panel) and digested with TseI (lower panel). DNA products were loaded on a 2% agarose gel. The red arrowhead marks the DNA band indicating HDR-

mediated correction, generated by TseI digestion. The blue arrowhead marks the DNA band of the uncorrected *mdx* allele. M denotes size marker lane. bp indicates the base pair length of the marker bands.

(B) Quantification of dystrophin-positive cells in quadriceps, soleus, diaphragm and heart. n= 6 for WT; n=3 for *mdx*. Error bars show standard deviation based on data from multiple muscle sections.

(C) Measurement of the distribution of the cross-sectional areas of myofibers from the soleus of wild-type mice showed uniformly sized fibers with 90% of the fibers ranging from 700-1499 μm^2. In contrast, myofibers from *mdx* mice were heterogeneous in size, ranging between 300-1899 μm^2. The size distribution of the myofibers from HDR-41% muscle was strikingly similar to that of wild-type mice. n= 6 for WT; n=3 for *mdx*. Error bars show standard deviation based on data from multiple muscle sections.

(D) Distribution of soleus myofibers with centralized nucleus. The percentage of regenerated myofibers of muscle from HDR-17% ranged from 700-1099 μm^2, which was higher than the percentage of fibers from the *mdx* muscle.

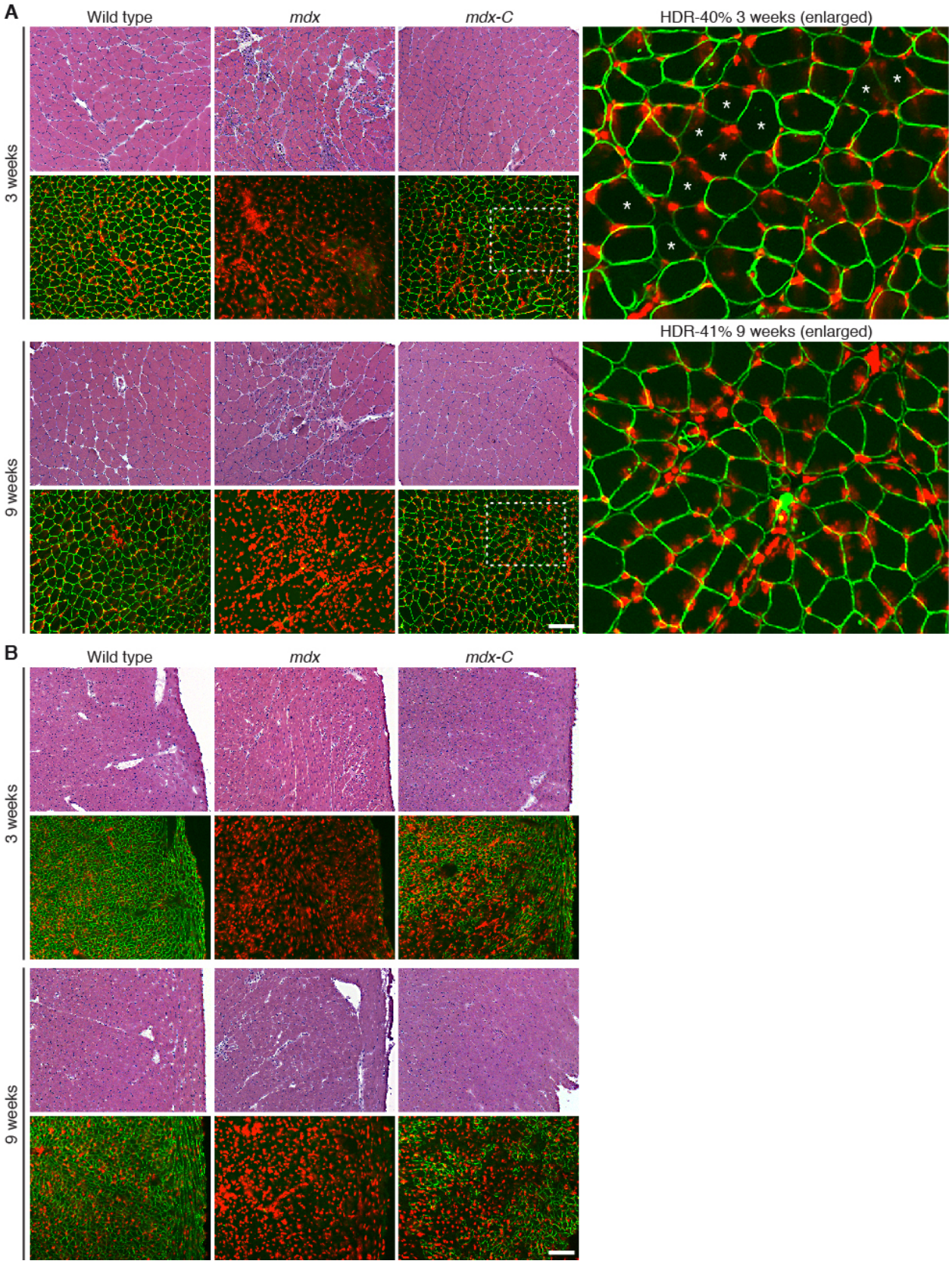
A
Wild type
mdx
mdx-C
HDR-40% 3 weeks (enlarged)
3 weeks
HDR-41% 9 weeks (enlarged)
9 weeks
B
Wild type
mdx
mdx-C
3 weeks
9 weeks

Fig. S7. Progressive recovery of skeletal muscle not heart following CRISPR/Cas9-mediated genomic editing of *Dmd* allele.

Hematoxylin and eosin (H&E) and dystrophin immunostaining of (**A**) soleus or **(B)** heart from 3-week old and 9-week old wild-type, *mdx, and mdx-C* mice (3-week-old is HDR-40%-3wk; 9-week old is HDR-41%). Immunofluorescence (green) detects dystrophin. Nuclei are labeled by propidium iodide (red). Magnification of boxed area shows 3-week old (HDR-40%-3wk) and 9-week old (HDR-41%) muscle. At 3-weeks of age many but not all of the myofibers express dystrophin showing partial recovery. White star indicates dystrophin-negative myofibers. By 9-weeks of age, all myofibers in the corrected muscle show dystrophin expression. **(B)** Although dystrophin expression has been restored in hearts of *mdx-C* mice, no progressive improvement with age is seen from 3-weeks to 9-weeks of age. Scale bar, 100 microns.

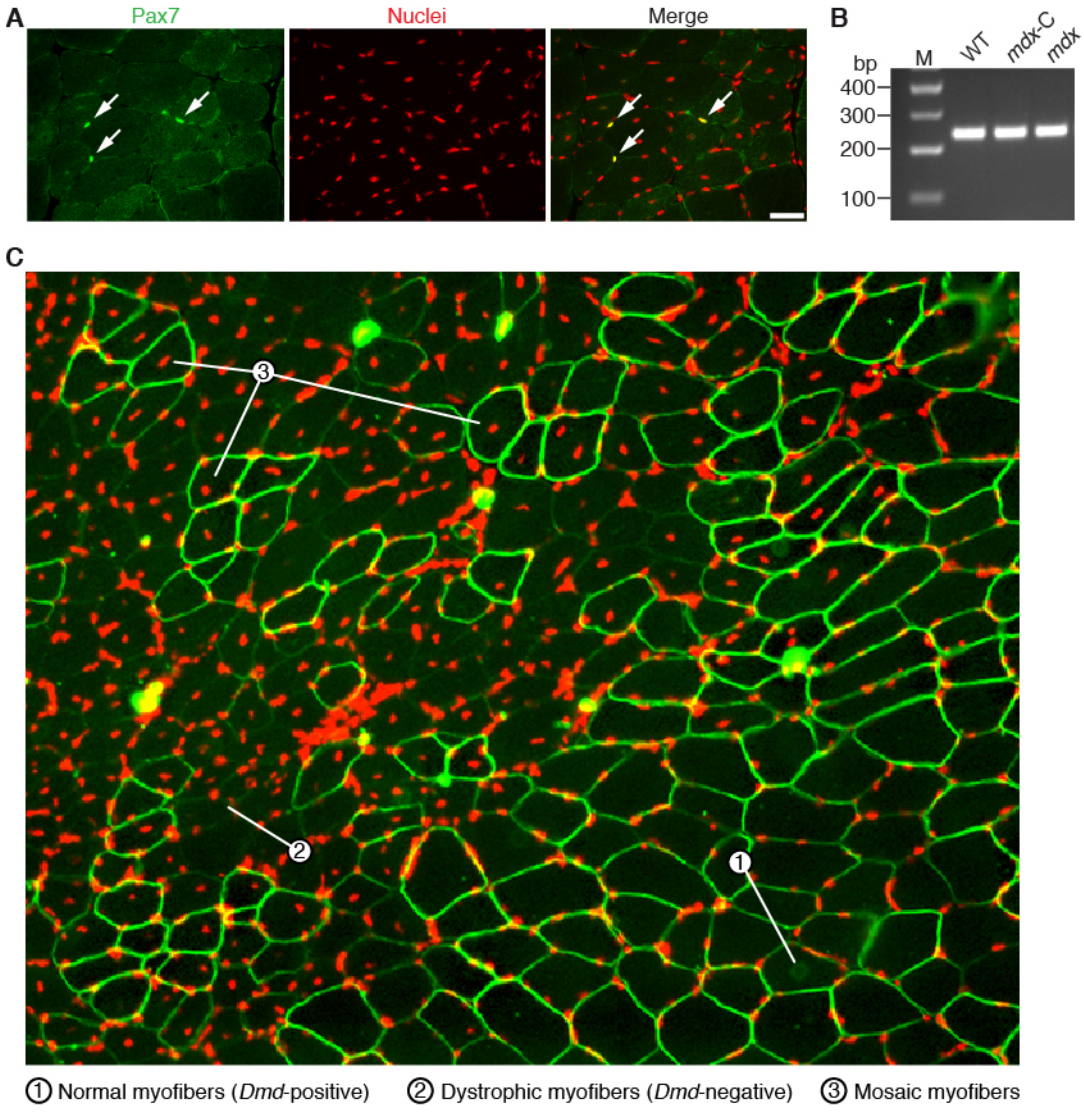

Fig. S8. Analysis of satellite cells and three types of myofibers in *mdx*-C mice.

(A) Cross-section of gastrocnemius from *mdx*-C mouse immunostained for satellite cell-specific marker, Pax7 (left, green) and nuclei (middle, red/propidium iodide). A merged image (right) shows the 'yellow' satellite cells located at the edges of the muscle fibers and distinguishes them from "red" myofiber nuclei. White arrows indicate Pax-7 positive satellite cells. Scale bar, 40 microns.

(B) The 232 bp PCR products corresponding to exon 23 of the *Dmd* gene from laser dissected satellite cells of wild-type, *mdx*-C and *mdx* mice were analyzed on a 2% agarose gel. M denotes size marker lane. bp indicates the base pair length of the marker bands.

(**C**) Immunostaining of *mdx*-C soleus with anti-dystrophin (green) and propidium iodide (red) highlighting three types of myofibers in the partially corrected *mdx* muscle: 1) normal dystrophin-positive myofibers that originated from CRISPR/Cas9-mediated genome-corrected muscle progenitors; 2) dystrophic dystrophin-negative myofibers that originated from *mdx* mutant progenitors; 3) mosaic dystrophin-positive myofibers with centralized nuclei that formed from fusion of corrected satellite cells with pre-existing dystrophic muscle.

Supplementary Tables

Table S1. Oligonucleotides and primer sequences.

ssODN used for HDR-medicated editing via embryo micro-injection	
Dmd_donor_TseI-s180	TGA TAT GAA TGA AAC TCA TCA AAT ATG CGT GTT AGT GTA AAT GAA CTT CTA TTT AAT TTT GAG GCT CTG CAA AGT TCT TTA AAG GAG CAG CAG AAT GGC TTC AAC TAT CTG AGT GAC ACT GTG AAG GAG ATG GCC AAG AAA GCA CCT TCA GAA ATA TGC CAG AAA TAT CTG TCA GAA TTT
Primers for genotyping	
Dmd_729F	gagaaacttctgtgatgtgaggacata
Dmd_729R	caatatctttgaaggactctgggtaaa
Primers for OT analysis	
DMD232_f	cttctatttaattttgaggctctgc
DMD232_r	cctgaaattttcgaagtttattcat
DS-OT-01_f	tatgccacttcttcaaagagatgat
DS-OT-01_r	aacaagcaaacaattcaaaggatag
DS-OT-02_f	aagaagatatggcattgctggta
DS-OT-02_r	tctggaaacaaaaaggcaatg
DS-OT-03_f	taagagttctgacatgatttccaca
DS-OT-03_r	tggaacactactctctacactgtgc
DS-OT-04_f	ctatgagtttaccaccctaatgtgc
DS-OT-04_r	cttatgcttgttcaggcaaatacc
DS-OT-05_f	ttttgagttgtgttcattttctgag
DS-OT-05_r	taggagtacagctgcttcttcagac
DS-OT-06_f	gaaaaacaaaattactgaggcatgt
DS-OT-06_r	cctccaagttcttatcttgtttgaa
DS-OT-07_f	agtgattttctgatgacccaaatta
DS-OT-07_r	tgtttttaatggctaggtgctaatc
DS-OT-08_f	tttcttggagctgtagtgtgtactg
DS-OT-08_r	ggaatagagtgagcattgttctgat
DS-OT-09_f	tgtcacagttgcaattcttagtgtt
DS-OT-09_r	cttagaaaaacaaggttcctgacaa
DS-OT-10_f	caataaggacaagtgaaggctaaaa
DS-OT-10_r	aggtctccacacatattcactcttc
DS-OTE-01_f	agatctgggagcttctatcaactg
DS-OTE-01_r	gggtagaagtgaatcaataagtgga
DS-OTE-02_f	gaacacttctttgcttctcatcact

DS-OTE-02_r	gctgagactactgtagccctttaga
DS-OTE-03_f	tagtttttcacattcagtccagctt
DS-OTE-03_r	gctttcaaaactacaccaaacctac
DS-OTE-04_f	ctttaaaatacaagcctccagttcc
DS-OTE-04_r	tatttgtttctcaaatttccagacc
DS-OTE-05_f	attttctagaggtggtctcacacac
DS-OTE-05_r	gaaaagtggatagacagtttcagga
DS-OTE-06_f	aacctaaaagaaaggacaaggagaa
DS-OTE-06_r	acatgactcggtaataaaccttgag
DS-OTE-07_f	ttgtaaaagttccaactcccagtag
DS-OTE-07_r	tttaaaatctatttccccagagagg
DS-OTE-08_f	tgtccatttttaacctgtgttctg
DS-OTE-08_r	ccctaactcagtttctcttgttctg
DS-OTE-09_f	atctgtgttttcaatgtggaatctt
DS-OTE-09_r	agaaagcgaataggatttcttgttt
DS-OTE-10_f	tcgaatcttctacaatatgcaatca
DS-OTE-10_r	gtgggaaatgtttcaagtatcacat
DS-OTE-11_f	gcaaaatacaacttctaagcaaacc
DS-OTE-11_r	ccagaccagaggtagagtgtttcta
DS-OTE-12_f	caggagtcagcctcttactttacaa
DS-OTE-12_r	gctagatgacaaagccacttaactc
DS-OTE-13_f	gctacagaaaagaggctaggaaagt
DS-OTE-13_r	gctttgaagatgccctagaaatact
DS-OTE-14_f	taatacataaggggacatcacgagt
DS-OTE-14_r	gatctttgtagtggtttttctcctg
DS-OTE-15_f	ttaagcggaaagataagctgaagta
DS-OTE-15_r	ggaccaatgttactggaacacatac
DS-OTE-16_f	cttctacattcacctccctgtgtt
DS-OTE-16_r	cccagcatctaagaaaggagtaata
DS-OTE-17_f	aaatttttagtcaaaagtgcttgga
DS-OTE-17_r	caataaacctttcagacttcattgg
DS-OTE-18_f	tatgatttccagggtaagtccacta
DS-OTE-18_r	gcacttttgctaacatctaaattcc
DS-OTE-19_f	aaagtatatctgagaatgccactgc
DS-OTE-19_r	gtagctgtaggaatgtctgtcctgt
DS-OTE-20_f	tgtaataaaatgagaatttgcacca
DS-OTE-20_r	aatgaagccaaggtacatacaaaga
DS-OTE-21_f	catgaagatacagaaacatcccagt
DS-OTE-21_r	ggagtggcaccctccttac
DS-OTE-22_f	ataccccaagccatacttgtatcat
DS-OTE-22_r	cacttatccatctaggaaagcagag

Table S2. Efficiency of CRISPR/Cas9-mediated genomic editing by cytoplasm and pronuclear injection.

Strain	Dose of Cas9/sgRNA/ssODN (μg/μl)	Injection Methods	No. of Transferred Zygotes	No. of Pups /Zygotes (%)	No. of Mutant Founders/Pups (%)	No. of HDR /Pups (%)
C57BL6/C3H	5/2.5/5	Nuc	60	29 (48%)	9 (31%)	1 (3.4%)
		Nuc+Cyt	60	27 (45%)	5 (19%)	1 (3.7%)
	10/5/5	Nuc	30	13 (43%)	1(7.7%)	1 (7.7%)
		Nuc+Cyt	30	17 (57%)	6(35%)	3 (18%)
C57BL/6	10/5/10	Nuc	48	9 (18%)	3 (33%)	1 (11%)
	50/20/10	Nuc+Cyt	30	12 (40%)	1 (8.3%)	0
mdx	10/10/10	Nuc	103	29 (28%)	4 (14%)	**1 (3.4%)**
		Nuc+Cyt	150	58 (39%)	7 (12%)	**4 (6.9%)**
	50/20/10	Nuc	30	14 (47%)	2 (6.7%)	**0**
		Nuc+Cyt	120	23 (19%)	9 (39%)	**2 (8.9%)**

Table S3. Sequences of the target site (*Dmd* exon 23) and 32 potential off-target (OT) sites in the mouse genome.

#	Target(20nt)-PAM(3nt)	locus (mm10)	score	mismatches	UCSC gene
DMD	TCTTTGAAAGAGCAACAAAATGG	chrX:83803318-83803340	37		
OT-01	TTTTTGAAAGAGCAACAATAAGG	chr16:53976196-53976218	5.5	2MMs [2:19]	
OT-02	TTTTTGAAAGATCAACAAAATAG	chr16:58084165-58084187	4.2	2MMs [2:12]	
OT-03	TCTGTGAAAGAGTAACAAAATGG	chr2:26068637-26068659	3.1	2MMs [4:13]	
OT-04	TCATTGAAAGAGCAACACAAGGG	chr17:85542328-85542350	2.6	2MMs [3:18]	
OT-05	TCTGAGAAATAGCAACAAAAGGG	chr5:28127468-28127490	2.3	3MMs [4:5:10]	
OT-06	TCTTTTAAAGAGCAACAATATGG	chr2:44769953-44769975	2.1	2MMs [6:19]	
OT-07	TCTTTGAAATAGGAACAAAACAG	chr14:93068307-93068329	2	2MMs [10:13]	
OT-08	GCTGTGAAAGAGCAACAAACAAG	chr9:95136798-95136820	1.5	3MMs [1:4:20]	
OT-09	TATTTAAAAAAGCAACAAAAAAG	chrX:45387898-45387920	1.5	3MMs [2:6:10]	
OT-10	TCTTTGAAAGTCCAACAAAAGAG	chr5:38571962-38571984	1.4	2MMs [11:12]	
OTE-01	ACTTTGAAAAAGCAACACAAAAG	chrX:169303124-169303146	0.6	3MMs [1:10:18]	NM_178754
OTE-02	TCTTTGAGAGAACAACAAACAGG	chr6:78381061-78381083	0.6	3MMs [8:12:20]	NM_011259
OTE-03	TCTTTGACAGAGAAACAAACAGG	chr16:10960046-10960068	0.5	3MMs [8:13:20]	NM_019980
OTE-04	ATTTTCAATGAGCAACAAAATGG	chr6:129053832-129053854	0.5	4MMs [1:2:6:9]	NR_024262
OTE-05	AATTTAAAAGAGAAACAAAATAG	chr2:118748097-118748119	0.4	4MMs [1:2:6:13]	NR_030716
OTE-06	TGTTTGAACCAGCAACAAATGAG	chr1:90830366-90830388	0.4	4MMs [2:9:10:20]	NM_001243008
OTE-07	TTTTTGAAAGAGAAGCAAAATAG	chr3:28668648-28668670	0.3	3MMs [2:13:15]	NM_026910
OTE-08	CCTTTGAGAGAACAACAAACAGG	chr8:109728362-109728384	0.3	4MMs [1:8:12:20]	NM_001080930
OTE-09	TTTATGAAACAGCAACAGAAAAG	chr2:76705331-76705353	0.3	4MMs [2:4:10:18]	NM_028004
OTE-10	TGTTAGAATGAGCAACAATACAG	chr2:126908236-126908258	0.3	4MMs [2:5:9:19]	NM_023220
OTE-11	TATTTAAAATAGGAACAAAAAAG	chr9:88581220-88581242	0.3	4MMs [2:6:10:13]	NM_001034906
OTE-12	TCATAGAAAGAGCAACCAATCAG	chr4:32723618-32723640	0.3	4MMs [3:5:17:20]	NM_001081392
OTE-13	TCTTGGAAAGAGGAAAAAAAGGG	chr19:26696234-26696256	0.2	3MMs [5:13:16]	NM_011416
OTE-14	TGTTTGTAAGGGAAACAAAAGGG	chr16:10170610-10170632	0.2	4MMs [2:7:11:13]	NM_026594
OTE-15	TCTTTCAAGCAGAAACAAAACAG	chr1:139447127-139447149	0.2	4MMs [6:9:10:13]	NM_172643
OTE-16	TCTGTGAAACAGTAACTAAACGG	chr5:134295459-134295481	0.2	4MMs [4:10:13:17]	NM_001080748
OTE-17	TCTTTGAAAGAGTATCTAAAAAG	chr2:79672854-79672876	0.1	3MMs [13:15:17]	NM_080558
OTE-18	TATATGAAAGAGCCACAAGATGG	chr10:20988803-20988825	0.1	4MMs [2:4:14:19]	NM_026203
OTE-19	TATTAGAAAGAGAAAGAAAAGAG	chr1:161837651-161837673	0.1	4MMs [2:5:13:16]	NM_172645
OTE-20	TCACTGAAAGAGCAAAGAAAGAG	chr16:48977882-48977904	0.1	4MMs [3:4:16:17]	NM_001110017
OTE-21	TCTCTGAAGGAACAACAACAAAG	chr7:45425042-45425064	0.1	4MMs [4:9:12:19]	NM_011304
OTE-22	TCTTTACAAGATCATCAAAAAAG	chr11:60875710-60875732	0.1	4MMs [6:7:12:15]	NM_001168507

Table S4. Deep sequencing results of PCR products from the *Dmd* target site.

Target Site	Group	HDR Reads	Del. Reads	In. Reads	Total Reads	NHEJ (indel) Freq %	HDR Freq %	Total Freq %
Dmd	**A: *mdx* control**	0	45	6	6623	0.77	0	**0.77**
	B: *mdx*+Cas9	1363	51	384	7975	5.45	17.09	**22.54**
	C: WT control	0	27	4	4663	0.66	0	**0.66**
	D: WT+Cas9	1211	1665	11	7024	23.86	17.24	**41.10**

Table S5. Deep sequencing results of PCR products from 32 potential off-target regions.

Site	Chr.	GroupA: *mdx* control				GroupB: *mdx*+Cas9				GroupC: WT control				GroupD: WT+Cas9			
		Del. Reads	In. Reads	Total Reads	Indel Freq %	Del. Reads	In. Reads	Total Reads	Indel Freq %	Del. Reads	In. Reads	Total Reads	Indel Freq %	Del. Reads	In. Reads	Total Reads	Indel Freq %
OT-01	16	6	1	1781	0.39	7	0	2811	0.25	3	1	1358	0.29	8	0	1732	0.46
OT-02	16	12	1	1797	0.72	16	0	2351	0.68	6	0	946	0.63	4	0	1243	0.32
OT-03	2	15	1	2196	0.73	11	0	4004	0.27	4	0	1729	0.23	4	1	1968	0.25
OT-04	17	27	16	4511	0.95	63	36	4101	2.41	30	16	4609	1.00	42	20	4074	1.52
OT-05	5	4	2	598	1.00	0	0	197	0.00	0	0	332	0.00	5	1	645	0.93
OT-06	2	13	2	2741	0.55	24	3	5516	0.49	6	0	2431	0.25	18	1	3191	0.60
OT-07	14	5	0	1527	0.33	7	2	3116	0.29	6	0	1504	0.40	4	1	1444	0.35
OT-08	9	55	12	8009	0.84	63	26	8018	1.11	70	2	7689	0.94	71	4	7925	0.95
OT-09	X	1	0	2075	0.05	3	1	2521	0.16	2	0	1911	0.10	0	0	2870	0.00
OT-10	5	2	0	2109	0.09	4	1	3606	0.14	2	1	1905	0.16	2	1	3129	0.10
OTE-01	X	0	0	653	0.00	2	0	1727	0.12	0	0	569	0.00	0	0	988	0.00
OTE-02	6	1	0	626	0.16	2	1	1669	0.18	0	0	490	0.00	4	0	873	0.46
OTE-03	16	5	0	1657	0.30	7	1	4304	0.19	0	0	1202	0.00	2	0	1733	0.12
OTE-04	6	13	4	3941	0.43	25	3	6546	0.43	10	0	2825	0.35	28	3	6524	0.48
OTE-05	2	0	0	563	0.00	1	0	774	0.13	1	0	480	0.21	1	0	860	0.12
OTE-06	1	10	0	2423	0.41	18	0	5763	0.31	7	0	4176	0.17	9	1	6277	0.16
OTE-07	3	2	0	854	0.23	5	0	1293	0.39	1	0	682	0.15	1	0	809	0.12
OTE-08	8	7	1	6815	0.12	13	5	8016	0.22	9	4	4835	0.27	12	1	6962	0.19
OTE-09	2	13	1	3080	0.45	8	0	4542	0.18	2	1	1017	0.29	7	1	3310	0.24
OTE-10	2	4	0	1323	0.30	7	0	1766	0.40	8	0	976	0.82	8	0	1760	0.45
OTE-11	9	3	0	402	0.75	0	0	350	0.00	0	0	428	0.00	2	0	619	0.32
OTE-12	4	9	2	2143	0.51	8	0	3246	0.25	4	0	1395	0.29	10	1	2496	0.44
OTE-13	19	0	0	1238	0.00	10	2	2930	0.41	4	0	1560	0.26	10	0	1240	0.81
OTE-14	16	1	0	1288	0.08	3	0	2515	0.12	0	0	693	0.00	2	1	944	0.32
OTE-15	1	0	0	607	0.00	4	0	1585	0.25	5	0	522	0.96	3	0	1048	0.29
OTE-16	5	11	1	2862	0.42	10	2	3560	0.34	18	2	4193	0.48	16	1	5952	0.29
OTE-17	2	3	0	1159	0.26	7	0	2216	0.32	0	0	1120	0.00	1	0	1533	0.07
OTE-18	10	4	0	1080	0.37	10	0	1933	0.52	2	0	639	0.31	6	0	1025	0.59
OTE-19	1	3	0	1173	0.26	13	0	2980	0.44	8	0	1101	0.73	5	1	1734	0.35
OTE-20	16	1	0	668	0.15	3	1	1274	0.31	2	0	669	0.30	2	0	1074	0.19
OTE-21	7	8	3	2157	0.51	22	2	4873	0.49	21	0	2425	0.87	20	1	3226	0.65
OTE-22	11	9	0	2828	0.32	9	2	4624	0.24	9	0	2423	0.37	5	1	3257	0.18
Total		247	47	66884	**0.44**	385	88	104727	**0.45**	240	27	58834	**0.45**	312	41	82465	**0.43**

References

1. R. J. Fairclough, M. J. Wood, K. E. Davies, Therapy for Duchenne muscular dystrophy: Renewed optimism from genetic approaches. *Nat. Rev. Genet.* **14**, 373–378 (2013). Medline doi:10.1038/nrg3460

2. R. G. Worton, M. W. Thompson, Genetics of Duchenne muscular dystrophy. *Annu. Rev. Genet.* **22**, 601–629 (1988). Medline doi:10.1146/annurev.ge.22.120188.003125

3. J. C. van Deutekom, G. J. van Ommen, Advances in Duchenne muscular dystrophy gene therapy. *Nat. Rev. Genet.* **4**, 774–783 (2003). Medline doi:10.1038/nrg1180

4. M. Jinek, K. Chylinski, I. Fonfara, M. Hauer, J. A. Doudna, E. Charpentier, A programmable dual-RNA-guided DNA endonuclease in adaptive bacterial immunity. *Science* **337**, 816–821 (2012). Medline doi:10.1126/science.1225829

5. L. Cong, F. A. Ran, D. Cox, S. Lin, R. Barretto, N. Habib, P. D. Hsu, X. Wu, W. Jiang, L. A. Marraffini, F. Zhang, Multiplex genome engineering using CRISPR/Cas systems. *Science* **339**, 819–823 (2013). Medline doi:10.1126/science.1231143

6. P. Mali, L. Yang, K. M. Esvelt, J. Aach, M. Guell, J. E. DiCarlo, J. E. Norville, G. M. Church, RNA-guided human genome engineering via Cas9. *Science* **339**, 823–826 (2013). Medline doi:10.1126/science.1232033

7. P. Mali, K. M. Esvelt, G. M. Church, Cas9 as a versatile tool for engineering biology. *Nat. Methods* **10**, 957–963 (2013). Medline doi:10.1038/nmeth.2649

8. F. D. Urnov, J. C. Miller, Y. L. Lee, C. M. Beausejour, J. M. Rock, S. Augustus, A. C. Jamieson, M. H. Porteus, P. D. Gregory, M. C. Holmes, Highly efficient endogenous human gene correction using designed zinc-finger nucleases. *Nature* **435**, 646–651 (2005). Medline doi:10.1038/nature03556

9. D. G. Ousterout, P. Perez-Pinera, P. I. Thakore, A. M. Kabadi, M. T. Brown, X. Qin, O. Fedrigo, V. Mouly, J. P. Tremblay, C. A. Gersbach, Reading frame correction by targeted genome editing restores dystrophin expression in cells from Duchenne muscular dystrophy patients. *Mol. Ther.* **21**, 1718–1726 (2013). Medline doi:10.1038/mt.2013.111

10. M. J. Osborn, C. G. Starker, A. N. McElroy, B. R. Webber, M. J. Riddle, L. Xia, A. P. DeFeo, R. Gabriel, M. Schmidt, C. von Kalle, D. F. Carlson, M. L. Maeder, J. K. Joung, J. E. Wagner, D. F. Voytas, B. R. Blazar, J. Tolar, TALEN-based gene correction for epidermolysis bullosa. *Mol. Ther.* **21**, 1151–1159 (2013). Medline doi:10.1038/mt.2013.56

11. Y. Wu, D. Liang, Y. Wang, M. Bai, W. Tang, S. Bao, Z. Yan, D. Li, J. Li, Correction of a genetic disease in mouse via use of CRISPR-Cas9. *Cell Stem Cell* **13**, 659–662 (2013). Medline doi:10.1016/j.stem.2013.10.016

12. G. Schwank, B. K. Koo, V. Sasselli, J. F. Dekkers, I. Heo, T. Demircan, N. Sasaki, S. Boymans, E. Cuppen, C. K. van der Ent, E. E. Nieuwenhuis, J. M. Beekman, H. Clevers, Functional repair of CFTR by CRISPR/Cas9 in intestinal stem cell organoids of cystic fibrosis patients. *Cell Stem Cell* **13**, 653–658 (2013). Medline doi:10.1016/j.stem.2013.11.002

13. H. Yin, W. Xue, S. Chen, R. L. Bogorad, E. Benedetti, M. Grompe, V. Koteliansky, P. A. Sharp, T. Jacks, D. G. Anderson, Genome editing with Cas9 in adult mice corrects a disease mutation and phenotype. *Nat. Biotechnol.* **32**, 551–553 (2014). Medline doi:10.1038/nbt.2884

14. G. Bulfield, W. G. Siller, P. A. Wight, K. J. Moore, X chromosome-linked muscular dystrophy (mdx) in the mouse. *Proc. Natl. Acad. Sci. U.S.A.* **81**, 1189–1192 (1984). Medline doi:10.1073/pnas.81.4.1189

15. P. Sicinski, Y. Geng, A. S. Ryder-Cook, E. A. Barnard, M. G. Darlison, P. J. Barnard, The molecular basis of muscular dystrophy in the mdx mouse: A point mutation. *Science* **244**, 1578–1580 (1989). Medline doi:10.1126/science.2662404

16. H. Wang, H. Yang, C. S. Shivalila, M. M. Dawlaty, A. W. Cheng, F. Zhang, R. Jaenisch, One-step generation of mice carrying mutations in multiple genes by CRISPR/Cas-mediated genome engineering. *Cell* **153**, 910–918 (2013). Medline doi:10.1016/j.cell.2013.04.025

17. H. Yang, H. Wang, C. S. Shivalila, A. W. Cheng, L. Shi, R. Jaenisch, One-step generation of mice carrying reporter and conditional alleles by CRISPR/Cas-mediated genome engineering. *Cell* **154**, 1370–1379 (2013). Medline doi:10.1016/j.cell.2013.08.022

18. S. T. Yen, M. Zhang, J. M. Deng, S. J. Usman, C. N. Smith, J. Parker-Thornburg, P. G. Swinton, J. F. Martina, R. R. Behringer, Somatic mosaicism and allele complexity induced by CRISPR/Cas9 RNA injections in mouse zygotes. *Dev. Biol.* 10.1016/j.ydbio.2014.06.017 (2014). doi:10.1016/j.ydbio.2014.06.017

19. X. Wu, D. A. Scott, A. J. Kriz, A. C. Chiu, P. D. Hsu, D. B. Dadon, A. W. Cheng, A. E. Trevino, S. Konermann, S. Chen, R. Jaenisch, F. Zhang, P. A. Sharp, Genome-wide binding of the CRISPR endonuclease Cas9 in mammalian cells. *Nat. Biotechnol.* **32**, 670–676 (2014). Medline doi:10.1038/nbt.2889

20. C. Kuscu, S. Arslan, R. Singh, J. Thorpe, M. Adli, Genome-wide analysis reveals characteristics of off-target sites bound by the Cas9 endonuclease. *Nat. Biotechnol.* **32**, 677–683 (2014). Medline doi:10.1038/nbt.2916

21. J. Duan, G. Lu, Z. Xie, M. Lou, J. Luo, L. Guo, Y. Zhang, Genome-wide identification of CRISPR/Cas9 off-targets in human genome. *Cell Res.* **24**, 1009–1012 (2014). Medline doi:10.1038/cr.2014.87

22. V. Pattanayak, S. Lin, J. P. Guilinger, E. Ma, J. A. Doudna, D. R. Liu, High-throughput profiling of off-target DNA cleavage reveals RNA-programmed Cas9 nuclease specificity. *Nat. Biotechnol.* **31**, 839–843 (2013). Medline doi:10.1038/nbt.2673

23. Y. Fu, J. A. Foden, C. Khayter, M. L. Maeder, D. Reyon, J. K. Joung, J. D. Sander, High-frequency off-target mutagenesis induced by CRISPR-Cas nucleases in human cells. *Nat. Biotechnol.* **31**, 822–826 (2013). Medline doi:10.1038/nbt.2623

24. S. R. Pigozzo, L. Da Re, C. Romualdi, P. G. Mazzara, E. Galletta, S. Fletcher, S. D. Wilton, L. Vitiello, Revertant fibers in the *mdx* murine model of Duchenne muscular dystrophy: An age- and muscle-related reappraisal. *PLOS ONE* **8**, e72147 (2013). Medline doi:10.1371/journal.pone.0072147

25. H. Yin, F. Price, M. A. Rudnicki, Satellite cells and the muscle stem cell niche. *Physiol. Rev.* **93**, 23–67 (2013). Medline doi:10.1152/physrev.00043.2011

26. D. Montarras, J. Morgan, C. Collins, F. Relaix, S. Zaffran, A. Cumano, T. Partridge, M. Buckingham, Direct isolation of satellite cells for skeletal muscle regeneration. *Science* **309**, 2064–2067 (2005). Medline doi:10.1126/science.1114758

27. A. C. Nathwani, C. Rosales, J. McIntosh, G. Rastegarlari, D. Nathwani, D. Raj, S. Nawathe, S. N. Waddington, R. Bronson, S. Jackson, R. E. Donahue, K. A. High, F. Mingozzi, C. Y. Ng, J. Zhou, Y. Spence, M. B. McCarville, M. Valentine, J. Allay, J. Coleman, S. Sleep, J. T. Gray, A. W. Nienhuis, A. M. Davidoff, Long-term safety and efficacy following systemic administration of a self-complementary AAV vector encoding human FIX pseudotyped with serotype 5 and 8 capsid proteins. *Mol. Ther.* **19**, 876–885 (2011). Medline doi:10.1038/mt.2010.274

28. M. A. Kotterman, D. V. Schaffer, Engineering adeno-associated viruses for clinical gene therapy. *Nat. Rev. Genet.* **15**, 445–451 (2014). Medline doi:10.1038/nrg3742

29. B. Peng, Y. Zhao, H. Lu, W. Pang, Y. Xu, In vivo plasmid DNA electroporation resulted in transfection of satellite cells and lasting transgene expression in regenerated muscle fibers. *Biochem. Biophys. Res. Commun.* **338**, 1490–1498 (2005). Medline doi:10.1016/j.bbrc.2005.10.111

30. M. S. Kormann, G. Hasenpusch, M. K. Aneja, G. Nica, A. W. Flemmer, S. Herber-Jonat, M. Huppmann, L. E. Mays, M. Illenyi, A. Schams, M. Griese, I. Bittmann, R. Handgretinger, D. Hartl, J. Rosenecker, C. Rudolph, Expression of therapeutic proteins after delivery of chemically modified mRNA in mice. *Nat. Biotechnol.* **29**, 154–157 (2011). Medline doi:10.1038/nbt.1733

31. L. Zangi, K. O. Lui, A. von Gise, Q. Ma, W. Ebina, L. M. Ptaszek, D. Später, H. Xu, M. Tabebordbar, R. Gorbatov, B. Sena, M. Nahrendorf, D. M. Briscoe, R. A. Li, A. J. Wagers, D. J. Rossi, W. T. Pu, K. R. Chien, Modified mRNA directs the fate of heart progenitor cells and induces vascular regeneration after myocardial infarction. *Nat. Biotechnol.* **31**, 898–907 (2013). Medline doi:10.1038/nbt.2682

32. T. J. Harris, J. J. Green, P. W. Fung, R. Langer, D. G. Anderson, S. N. Bhatia, Tissue-specific gene delivery via nanoparticle coating. *Biomaterials* **31**, 998–1006 (2010). Medline doi:10.1016/j.biomaterials.2009.10.012

33. P. D. Hsu, E. S. Lander, F. Zhang, Development and applications of CRISPR-Cas9 for genome engineering. *Cell* **157**, 1262–1278 (2014). Medline doi:10.1016/j.cell.2014.05.010

34. L. V. Nicholson, K. Davison, G. Falkous, C. Harwood, E. O'Donnell, C. R. Slater, J. B. Harris, Dystrophin in skeletal muscle. I. Western blot analysis using a monoclonal antibody. *J. Neurol. Sci.* **94**, 125–136 (1989). Medline doi:10.1016/0022-510X(89)90223-2

35. K. Kodippili, L. Vince, J. H. Shin, Y. Yue, G. E. Morris, M. A. McIntosh, D. Duan, Characterization of 65 epitope-specific dystrophin monoclonal antibodies in canine and murine models of Duchenne muscular dystrophy by immunostaining and western blot. *PLOS ONE* **9**, e88280 (2014). Medline doi:10.1371/journal.pone.0088280

36. M. M. Murphy, J. A. Lawson, S. J. Mathew, D. A. Hutcheson, G. Kardon, Satellite cells, connective tissue fibroblasts and their interactions are crucial for muscle regeneration. *Development* **138**, 3625–3637 (2011). Medline doi:10.1242/dev.064162

37. L. M. Gjerdrum, I. Lielpetere, L. M. Rasmussen, K. Bendix, S. Hamilton-Dutoit, Laser-assisted microdissection of membrane-mounted paraffin sections for polymerase chain reaction analysis: Identification of cell populations using immunohistochemistry and in situ hybridization. *J. Mol. Diagn.* **3**, 105–110 (2001). Medline doi:10.1016/S1525-1578(10)60659-9